Chapter 8 Environmental Effects on Space Systems

A Spacecraft Charging

1 Introduction

Spacecraft charging results from the interaction of satellites with charged particles and energetic photons in the space environment. Two classes of phenomena are of interest:

(a) Surface charging
(b) Internal charging

These processes lead to a variety of operational anomalies as listed.

(a) Degradation of surfaces including sensor surfaces
(b) Interference in electrical circuits due to arcing
(c) Internal charge accumulations in electronic components

Some of these effects can have serious consequences including loss of the spacecraft or mission objectives.

2 Charging Mechanisms

While there are several mechanisms which contribute to spacecraft charging, the three most important ones are

(a) Charge flow from the ambient plasma
(b) Photoelectron emission from the spacecraft
(c) Secondary emission due to plasma bombardment

These currents produce a current flow to the satellite, and generally result in a non-zero charge on the satellite body (and surfaces), and hence non-zero potentials. These potentials can be *quite* large. The general scenario is presented in figure 8.1, where the different current sources are identified.

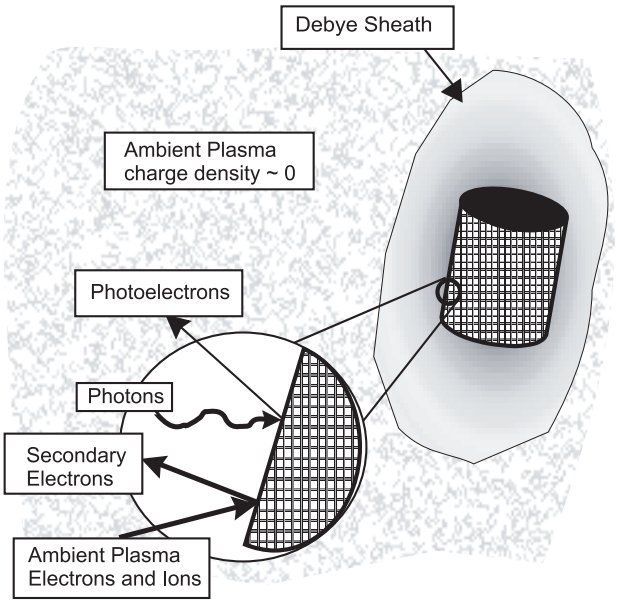

Figure 8.1. Spacecraft Charging Processes. Note that the charge distribution near the satellite can be non-neutral, and in the case of actively biased systems (such as near solar arrays), extremely non-neutral.

Plasma Induced Charging

In a plasma, charge neutrality is maintained by strong, long range electric forces. This generally requires that on average, the electron and (positive) ion densities are equal (quasi-neutrality). The average kinetic energies (temperatures) are often similar. In general, their velocities are quite different, however. This can be seen if we go ahead and assume that both electrons and ions (usually protons) are at the same temperature.

The thermal velocity is given by:

$$< E >= \frac{3}{2}kT = \frac{1}{2}m_e v_e^{\,2} = \frac{1}{2}m_i v_i^{\,2}. \qquad \text{(Eqn. 8.1)}$$

Assuming that most ions are protons, we see that the ratio of thermal velocities is fairly high:

$$\frac{v_e}{v_i} = \sqrt{\frac{m_i}{m_e}} = \sqrt{\frac{m_p}{m_e}} = 43 \qquad \text{(Eqn. 8.2)}$$

Hence the electron velocity is much higher than the ion velocity. In the simplest case (no effects due to satellite motion or plasma flow), the current density (current/area) incident on a satellite surface is given by:

$$j = qnv \qquad \text{(Eqn. 8.3)}$$

where:
q = charge on particle (Coulombs)
n = particle density (number/m^3)
v = (thermal) velocity (m/s)

Since the charge and density are the same, we see that the current density is much higher for the electrons than the ions (43 times higher, for a proton plasma). (Study question - what is the ratio for an oxygen (O+) environment ?)

Example
Typical values of $kT_e = kT_i = 8000$eV at Geosynchronous orbit. Typical densities are about 10^6 particles/m^3 and $q = \pm 1.6 \times 10^{-19}$ C, yielding for the velocities

$$v_e = \sqrt{\frac{kTe}{m_e}} = \sqrt{\frac{8000 \times 1.6 \times 10^{-19}}{9.1 \times 10^{-31}}} = 3.75 \times 10^7 \ {}^{m}\!/_{sec} \qquad \text{(Eqn. 8.4a)}$$

$$v_p = \sqrt{\frac{kTe}{m_p}} = \sqrt{\frac{8000 \times 1.6 \times 10^{-14}}{1.6 \times 10^{-27}}} = 8.67 \times 10^5 \ {}^{m}\!/_{sec} \qquad \text{(Eqn. 8.4b)}$$

and the resulting current densities are:

$$j_e = -n_e e v_e = -\left(10^6\right)\left(1.6 \times 10^{-19}\right)\left(3.75 \times 10^7\right) = -6\text{x}10^{-6}\left({}^{A}\!/_{m^2}\right) \qquad \text{(Eqn. 8.5a)}$$

$$j_p = +n_p e v_p = +\left(10^6\right)\left(1.6 \times 10^{-19}\right)\left(8.67 \times 10^5\right) = +1.3\text{x}10^{-7}\left({}^{A}\!/_{m^2}\right) \qquad \text{(Eqn. 8.5b)}$$

for the electrons and protons incident on the spacecraft

Typical cross-sectional areas are 5 m^2, so the net current is

$$\begin{aligned} I_{net} &= \left(j_{net}\right)(\text{Area}) = (j_e + j_p)(\text{Area}) \\ &= \left(-6 \times 10^{-6} + 1.3 \times 10^{-7}\right)(5) = -2.9 \times 10^{-5}(\text{Amp}) \end{aligned} \qquad \text{(Eqn. 8.6)}$$

Because of this negative charge accumulation, a net potential develops on the satellite. Using our example, in one millisecond, a charge $\Delta q = (I_{net})(t) = -2.9\text{x}10^{-8}$ C develops. If the capacitance is 100 pF (a typical value), a potential of $V = q/C = -0.29$ kV is developed. (The capacitance can be estimated by assuming the satellite is a sphere - see Halliday and Resnick - C(picoFarads) ~ radius (cm))

This potential reduces the incident electron flux until it is balanced by the ion flux. The mathematics of this process is fairly simple, but one must do a little kinetic theory to obtain the effect of the potential on the currents. For the repelled specie ($q\Phi > 0$):

$$I = I_o e^{{}^{q\phi}\!/_{kT}} \qquad \text{(Eqn. 8.7a)}$$

and for the attracted specie ($q\Phi < 0$):

$$I = I_o \left(1 - \frac{q\Phi}{kT}\right) \qquad \text{(Eqn. 8.7b)}$$

where $I_o = qnvA$.

Equilibrium occurs when there is no net current - then the potential stops changing. This point can be determined by setting the two terms for current above equal to each other. Roughly, this tends to occur when the potential energy of the electrons is roughly equal to their average kinetic energy.

$$-e\Phi_S \cong kT \Rightarrow \Phi_S = -\frac{kT}{e} \qquad \text{(Eqn. 8.8)}$$

where Φ_s = spacecraft potential (Volts). The electron flux is then substantially reduced, and the ion current is increased slightly. This relation holds reasonably true in the absence of other current sources, which as a practical matter tends to mean LEO, in eclipse.

Otherwise, there are several additional current sources which are important. The largest of these is photoemission.

Photoelectric Emission

When photons of sufficient energy strike a material surface electrons are ejected from the surface leaving the target positively charged. This process can be represented as shown

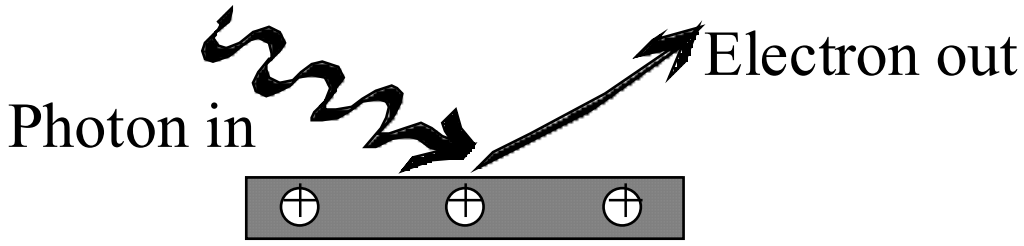

Figure 8.2 Photoemission

The energy balance in this process can be written

$$hf = \varnothing + Ke_e \qquad \text{(Eqn. 8.9)}$$

where hf = Energy of incident photon
$\varnothing$ = Work function of the material
KE_e = Kinetic energy of ejected electron

As can be seen in Table 1 the work functions of most spacecraft materials are about 4-5 eV which means that only photons in the UV and X-Rays region $(\lambda \le 300\text{nm})$ can generate photoelectrons. Nevertheless because of the intense fluxes of UV and soft X-Rays (particularly the Lyman-alpha) in the solar spectrum this is an important mechanisms for positive charging of spacecraft. Since this mechanism is operative only when the spacecraft is in sunlight it results in a cycling of the spacecraft charge for orbiting satellites that pass in and out of eclipse. (Compare the values in Table 8.1 to the current densities calculated in equation 8.5.)

Table 8.1

Material	Work Function (eV)	Photoelectron Saturation Flux (10^{14}/sec-m^2)	Saturation Current Density (μA/m^2)
Aluminum Oxide	3.9	260	42
Indium Oxide	4.8	190	30
Gold	4.8	180	29
Stainless Steel	4.4	120	20
Aquadag	4.6	110	18
LiF on Au	4.4	90	15
Vitreous Carbon	4.8	80	13
Graphite	4.7	25	4

Secondary Emission

Finally. there are substantial currents generated by the incident particles. Incident electrons with energies of a few hundred electron volts (100-500 eV) will produce secondary electrons. These secondary electrons escape the surface with energies of a few eV, and their energy spectrum resembles that of the photoelectrons. For some materials, the secondary electron yield can exceed one. This can lead to the anomalous result of having a net positive current produced by the incident electron flux. As the plasma temperature increases, this net secondary yield decreases, typically at temperatures exceeding 10 KeV. (That is, one needs a substantial number of electrons with energies over 10 KeV in order for a net negative charge to flow to the satellite, even in eclipse.)

3 Example of Spacecraft Charging – Geosynchronous Orbit

For geosynchronous satellites, spacecraft charging divides itself into two regimes - sunlight and eclipse (shadow). In hot plasma environments, a conducting satellite will experience positive potentials in sunlight, negative potentials in eclipse.

The above discussion assumes that the satellite surface is conducting. This is not typically true, since the materials covering a satellite usually include glass (SiO_2 cover cells on the solar arrays) and kapton (thermal blanket). This is important because shadowed, insulating surfaces can develop large negative potentials (hundreds to thousands of volts), even though the illuminated surfaces and satellite ground have small positive potentials. This “differential charging” can lead to arcing on the satellite surface. These arcs lead to electrical pulses which can couple into the satellite command and control circuitry, leading to anomalous satellite behavior

CHARGING CONDITIONS IN GEOSYNCHRONOUS ORBIT

a) ECLIPSE - NEGATIVE CHARGING b) SUNLIGHT - POSITIVE CHARGING

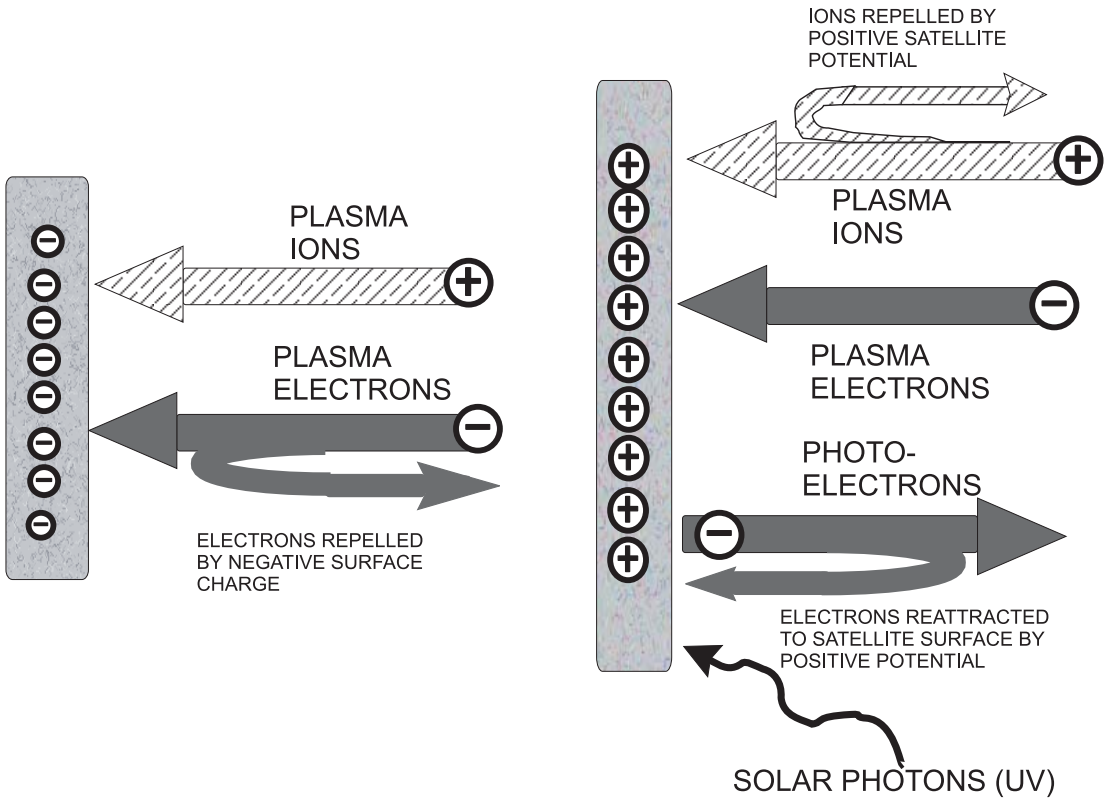

Figure 8.3. Qualitative illustration of the charging of a surface by a plasma. The width of the arrows is proportional to the flux of each particle species; the equilibrium potential is reached when the sum of the currents collected and emitted by a surface element s zero. (a) Surface in shadow: the current balance requires equality between the flow of the plasma ions and that of the electrons impinging on the surface. (b) Surface in sunlight: equilibrium is achieved when the flow of escaping photoelectrons is equal to the difference between the incoming flows of plasma electrons and ions.

As a special illustration of the magnitudes of charging which can be experienced at geosynchronous orbit, the record charging event from Applied Technology Satellite 6 is shown in Figures 8.4 and 8.5. Figure 8.4 is a spectrogram for a two hour interval in 1975, covering an eclipse. This figure is similar in spirit to that shown in chapter 5, but the energy range is substantially larger, extending upwards to 80 keV. The eclipse begins just prior to 2100, and ends just before 2200. There is an injection of hot plasma about 10 minutes into the eclipse, and the satellite potential reaches -19 kV. Other satellites have not been observed to charge to such levels - we were just lucky.

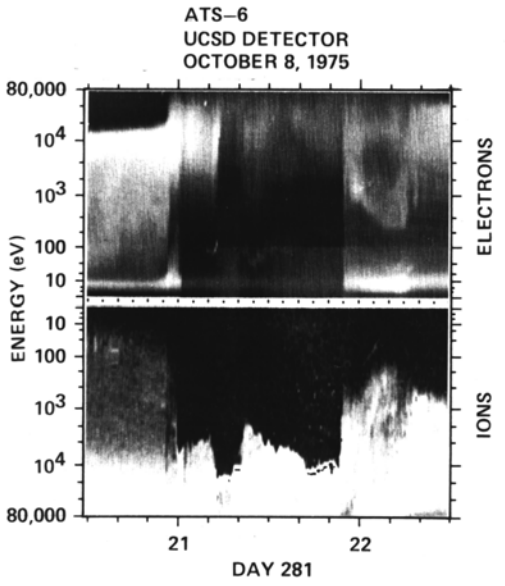

Figure 8.5. Ion and electron spectrogram for the record charging event. Note that by definition, the event occurs at local midnight, typically a region of relatively hot plasmas. The electron energies reach (and apparently exceed) 80 keV.

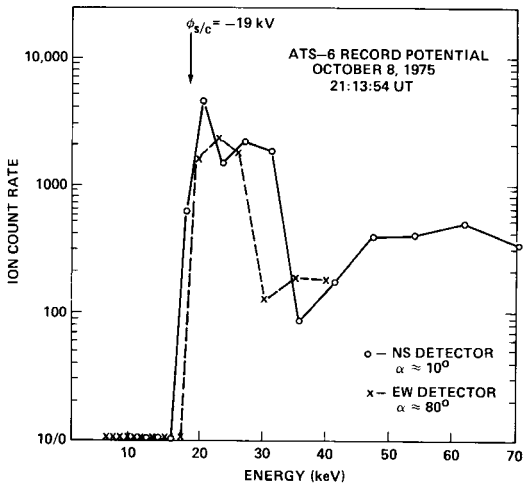

Figure 8.5. Ion spectra for the record charging event.

4 Design Considerations

There are two classes of solutions to minimize spacecraft charging:

(a) To prevent differential charging assure to the extent possible that the entire surface is of uniform conductivity. (Covering solar cells with a transparent but conducting film of Indium oxide is an example).
(b) Prevent establishment of large potentials by installing plasma generating devices or plasma jets which can actively balance currents to spacecraft surfaces. The devices are often called "plasma contactors" and they effectively "ground" the spacecraft to the surrounding plasma by emitting beams of electrons or ions.

Generally, the above solutions have only been adopted on NASA science mission, operational, DoD, mission and commercial satellites have not generally implemented those solutions. Instead, a set of engineering solutions have been adopted. Most notably, cables should not be run outside the satellite body except where absolutely necessary. Multiple ground loops must be eliminated. Critical command circuitry is designed to not trigger on single pulses.

B Orbital Debris

1 Space Operations and Orbital Debris

We begin our look at this problem with the first chapter from a recently issued report by the Committee on Space Debris of the National Research Council called:

Orbital Debris - A Technical Assessment
National Academy Press, (1995)
2101 Constitution Ave., Washington DC 20418

Space Operations

In the 37 years since the launch of Sputnik 1, space operations have become an integral component of the world's economy, scientific activities, and security systems. Orbital debris is inextricably linked with these operations: debris is created in the course of these operations and is important because it poses a potential threat to future operations. Understanding some of the characteristics of historical, current, and future space operations is thus essential to understanding the overall debris problem.

Today, spacecraft owned by 23 nations and several international organizations (representing more than 100 countries) support a wide variety of important missions, including communications, navigation, meteorology, geodesy and geophysics, remote sensing, search and rescue, materials and life sciences, astrophysics, and national security. A broad spectrum of simple and sophisticated functional spacecraft, with masses ranging from tens of kilograms to tens of metric tons and operational lives ranging from one week to more than ten years are employed to carry out these space activities.

These spacecraft are placed into orbit by a wide variety of launch vehicles. These launch vehicles, which may be either solid or liquid fueled, use multiple stages (some of which may themselves go into orbit) to place spacecraft into their desired orbit. Some spacecraft retain the stage used to perform their orbital insertion maneuver, and most spacecraft have some propulsive capability for attitude control and performing orbital corrections. These spacecraft are placed into orbits from which they can accomplish their particular mission effectively, resulting in a highly non-uniform distribution of spacecraft about the Earth. A few spacecraft each year are launched out of Earth orbit and into interplanetary space; the hazard to future space operations from these probes is utterly negligible.

The distribution of spacecraft around the Earth at the start of 1994 is displayed in Figure 8-5. This distribution is not static; as missions, technologies, and available launch vehicles change, the distribution of functional spacecraft also changes. For example, over the past three decades, the annual percentage of new space missions to orbits above LEO has been increasing; in 1993, High Earth Orbits (HEOs) were the final destination of 42 percent of successful launchings worldwide. Proposed future constellations of communications spacecraft in LEO may reverse this trend.

Figure 8.6 reveals a few characteristics of the current spacecraft population. Most spacecraft reside in LEO, but there are three significant concentrations in higher orbits. There is a concentration of spacecraft (performing Earth observation and communications missions) in

GEO. A second concentration in and near circular semisynchronous orbits is made up of spacecraft from the U.S. Global Positioning System (GPS) and the Russian Global Navigation Satellite System. There is also a significant population of spacecraft in highly elliptical Molniya-type orbits, including Commonwealth of Independent States (CIS) early warning and communications constellations. (In this report, we will refer to pre-1992 space activities of the former USSR as "Soviet" and those of 1992 and later as either "Russian" or of the CIS, as appropriate.) In LEO, notable peaks exist around 1,400 to 1,500 km (due in part to a constellation of Russian communication spacecraft and debris from three breakups of Delta rocket bodies) and 900 to 1,000 km (due in part to Sun-synchronous remote sensing and navigation spacecraft and their associated debris).

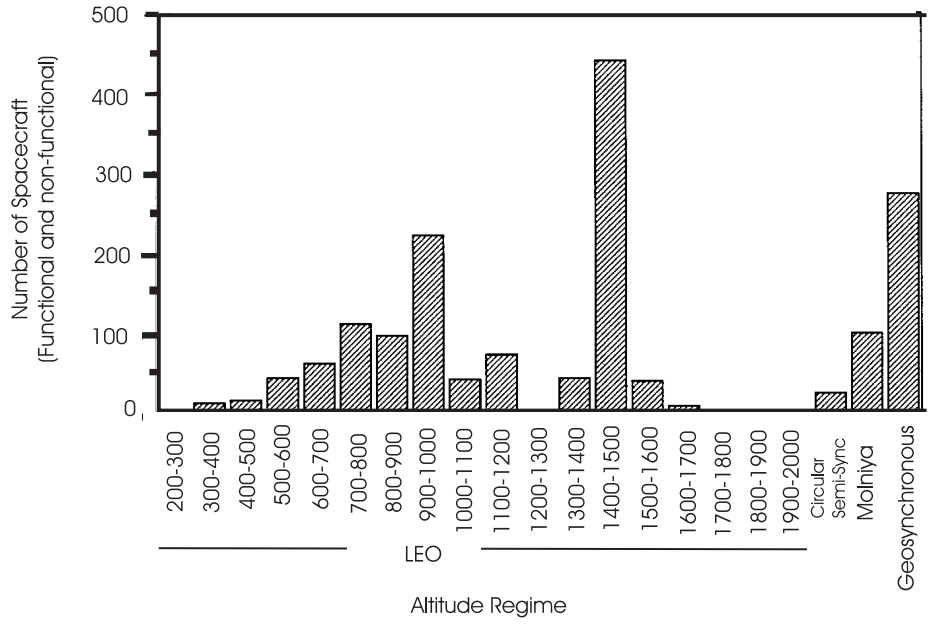

Figure 8.6. Spacecraft population in Earth orbit, 1994.

Most space activities involving humans occur below about 600 km; there are currently few spacecraft in these low orbits because atmospheric drag at these altitudes causes fairly rapid orbital decay.

Table 8.2
Debris Size Conventions - This report user three general size ranges to categorize debris

Size Category	Approximate Diameter	Approximate Mass	Estimated Number	Detectability	Probable Damage to Spacecraft
Large	>10 cm	>1 kg	8,000	May be catalogable in LEO	Probable loss of spacecraft and possible catastrophic breakup
Medium	1 mm - 10 cm	1 mg - 1 kg	10^7 - 10^8	Too small to catalog, too few for most in situ sampling	Ranges from surface degradation through component damage and loss of spacecraft capability
Small	< 1 mm	< 1 mg	10^{12}	Detectable by in situ sampling	Degradation of surface and possible damage to unprotected components

Types of Orbital Debris

The more than 3,600 space missions since 1957 have left a legacy of thousands of large and perhaps tens of millions of medium-sized debris objects in near-Earth space. Unlike meteoroids, which pass through and leave the near-Earth area, artificial space debris orbit the Earth and may remain in orbit for long periods of time. Of the 23,000 space objects officially cataloged by the U.S. Space Surveillance Network (SSN) since the beginning of space age, nearly one-third remain in orbit about the Earth; the majority of these are expected to stay in orbit for tens or hundreds of years. The increasing population of cataloged space objects is represented in Figure 8.7. It is imperative to note that this figure shows only the objects large enough to be repeatedly tracked by ground-based radar. The vast majority of debris is too small to be tracked and is not represented.

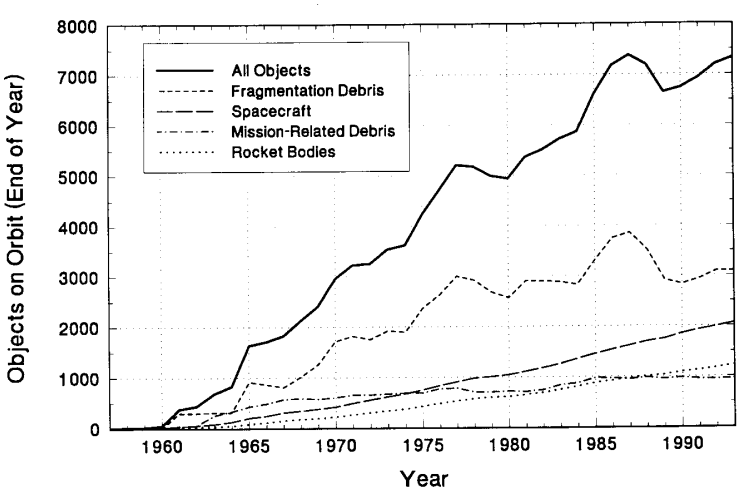

Figure 8.7. On-Orbit cataloged population (corrected for delayed cataloging).

Objects in Earth orbit that are not functional spacecraft are considered debris. Spacecraft that are passive, serving as platforms for laser ranging experiments, atmospheric density measurements, or calibration of space surveillance sensors are considered functional, as are spacecraft that are currently in a reserve or standby status and may be reactivated in the future to continue their mission. Each other type of object in Earth orbit may be classified as belonging to one of four types of debris: nonfunctional spacecraft, rocket bodies, mission-related debris, and fragmentation debris. Figure 8.8 indicates the relative numbers of cataloged functional spacecraft and debris as of March 1994. More than 90% of these cataloged space objects are of U.S. or Soviet/CIS origin, while the remainder belong to nearly 30 other countries or organizations.

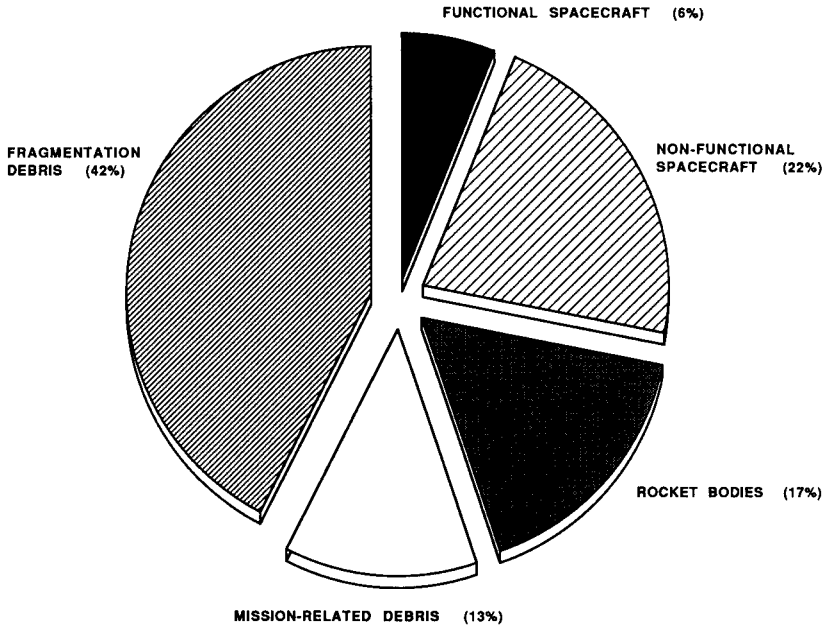

Figure 8.8. Cataloged space objects by category, 1994.

Nonfunctional Spacecraft

Functional spacecraft represent only about one-fifth of the spacecraft population in Earth orbit - the large majority of orbiting spacecraft are nonfunctional. With very few exceptions, functional spacecraft that reach their end of life (EOL), through either termination or malfunction, are left in their former orbit or are transferred to slightly higher or lower altitudes (i.e., are reorbited). Typically, EOL reorbiting maneuvers are performed only by Geosynchronous or semisynchronous spacecraft and by LEO spacecraft carrying nuclear materials. Historically, these EOL maneuvers have almost always resulted in longer orbital lifetimes. Only crewed vehicles and a few other spacecraft (e.g., reconnaissance or space station related) in very low orbits are normally returned to Earth at the conclusion of their missions.

Rocket Bodies

The majority of functional spacecraft are accompanied into Earth orbit by one or more stages (or "rocket bodies") of the vehicles that launched them. Usually only one rocket body is left in orbit for missions to LEO, but the launch vehicle of a high-altitude spacecraft such as GEOS (Geostationary Operational Environmental Satellite) may release up to three separate rocket bodies in different orbits along the way to its final destination. Relatively few spacecraft types (e.g., the U.S. National Oceanic and Atmospheric Administration and Defense Meteorological Satellite Program meteorological spacecraft and Soviet nuclear-powered ocean reconnaissance spacecraft) are designed to retain their orbital insertion stages and leave no independent rocket bodies. Figure 8.9 depicts the rocket bodies and other large debris placed into various orbits in the course of a Proton launch vehicle's delivery of a payload to GEO.

The presence of rocket bodies in orbit is of particular importance to the future evolution of the Earth's debris population due to their characteristically large dimensions and to the potentially explosive residual propellants and other energy sources they may contain. Although the largest stages, which are generally used to deliver spacecraft and any additional stages into LEO, usually reenter the atmosphere rapidly, smaller stages used to transfer spacecraft into higher orbits and insert them into those orbits remain in orbit for long periods of time. Many of these rocket bodies are in orbits that intersect those used by functional spacecraft.

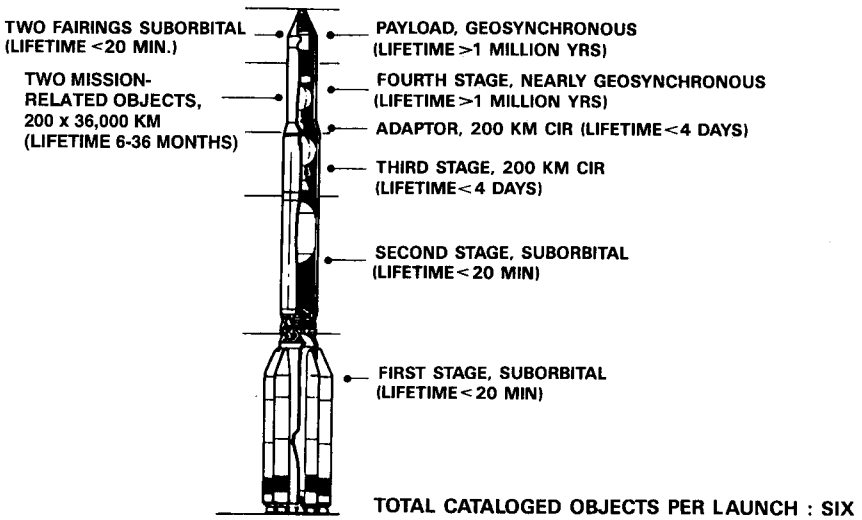

Figure 8.9. Typical debris produced in a Proton launch to GEO.

Mission-Related Debris

Other space objects, referred to as mission-related debris, may be released as a result of a spacecraft's deployment, activation, and operation. Parts of explosive bolts, spring release mechanisms, or spin-up devices may be ejected during the staging and spacecraft separation process. Shortly after entering orbit, the spacecraft may release cords securing solar panels and other appendages or eject protective coverings from payload and attitude control sensors. The amount of debris released can be quite large; a detailed study of the debris released by one Russian launch mission revealed that 76 separate objects were released into orbit from either the launch vehicle or the spacecraft. Numerous debris may also be created during a spacecraft's active life. For example, during the first four years of its operation, more than 200 pieces of mission-related debris linked with the Mir space station were cataloged. Although the occasional item accidentally dropped by a cosmonaut or astronaut may be newsworthy, the majority of this type of debris is intentionally dumped refuse. Since mission-related debris are often relatively small, only the larger items can be detected and cataloged by present-day ground-based surveillance networks.

Another type of mission-related debris comes from the operation of solid rocket motors normally used as final transfer stages, particularly on GEO missions. Current solid rocket fuel usually employs significant quantities of aluminum mixed with the propellant to dampen burn rate instabilities. However, during the burning process, large numbers of aluminum oxide (Al_2O_3) particles are formed and ejected through a wide range of flight path angles at velocities up to 4 km/s. These particles are generally believed to be no larger than 10 microns in diameter, but as many as 10^{20} may be created during the firing of a single solid rocket motor, depending on the distribution of sizes produced. While the orbital lifetimes of individual particles are relatively short, a considerable average population is suggested by examinations of impacts on exposed spacecraft surfaces. More than 25 solid rocket motor firings were conducted in orbit during 1993.

More recently, attention has been drawn to another side effect of solid rocket motors. Ground tests indicate that in addition to the large number of small particles, a smaller number of 1-cm or larger lumps of Al_2O_3 are also ejected during nominal burns. The only indication of the existence of such objects are data from ground tests carried out at Marshall Space Flight Center, Alabama, and the Arnold Engineering and Development Center (Siebold et al., 1993). These medium-sized particles, which have lower characteristic ejection velocities and smaller area-to-mass ratios than the smaller particles, may also be longer-lived than the small particles and could pose a long-term hazard to other Earth-orbiting space objects.

Fragmentation Debris

Fragmentation debris - the single largest element of the cataloged Earth-orbiting space object population - consists of space objects created during breakups and the products of deterioration. Breakups are typically destructive events that generate numerous smaller objects with a wide range of initial velocities. Breakups may be accidental (e.g., due to a propulsion system malfunction) or the result of intentional actions (e.g., space weapons tests). They may be caused by internal explosions or by an unplanned or deliberate collision with another orbiting object.

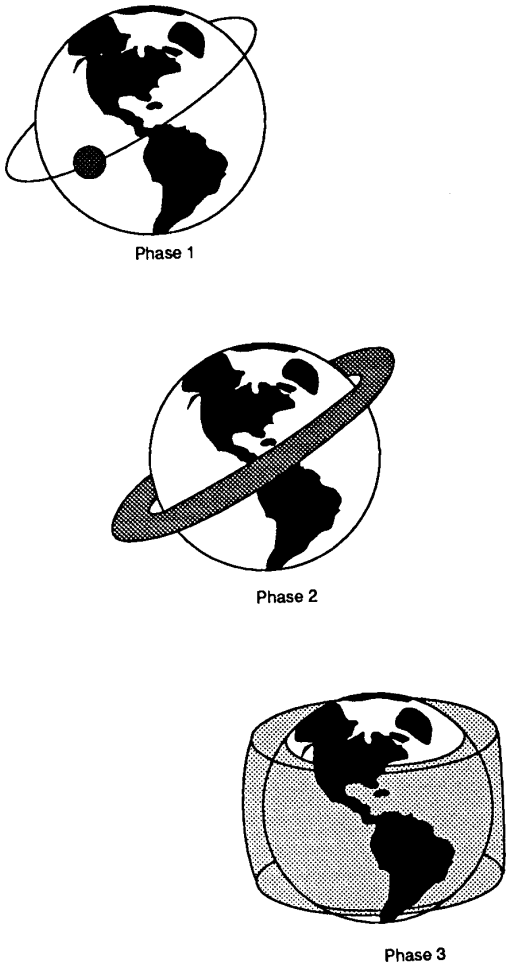

Since 1961, more than 120 known breakups have resulted in approximately 8,100 cataloged items of fragmentation debris, more than 3,100 of which remain in orbit. Fragmentation debris thus currently makes up more than 40 percent of the U.S. space object catalog (and undoubtedly represents an even larger fraction of non-cataloged objects). The most intensive breakup on record was the 1987 breakup of the Soviet Kosmos 1813, which generated approximately 850 fragments detectable from the Earth. The fragmentation debris released from a breakup will be ejected at a variety of initial velocities. As a result of their varying velocities, the fragments will spread out into a toroidal cloud that will eventually expand until it is bounded only by the limits of the maximum inclinations and altitudes of the debris. This process is illustrated in Figure 8-10. The rate at which the toroidal cloud evolves depends on both the original spacecraft's orbital characteristics and the velocity imparted to the fragments; in general, the greater the spread of the initial velocity of the fragments, the faster will the evolution occur.

Figure 8.10. Evolution of a debris cloud.

In contrast, debris fragments that are the product of deterioration usually separate at low relative velocity from a spacecraft or rocket body that remains essentially intact. Products of deterioration large enough to be detected from Earth are occasionally seen - probably such items as thermal blankets, protective shields, or solar panels. Most such deterioration is believed to be the result of harsh environment factors, such as atomic oxygen, radiation, and thermal cycling. During 1993 the still-functional COBE (Cosmic Background Explorer) spacecraft released at least 40 objects detectable from Earth - possibly debonded thermal blanket segments - in a nine-month period, perhaps as a result of thermal shock.

Another serious degradation problem involves the flaking of small paint chips as a space object ages under the influence of solar radiation, atomic oxygen, and other forces. Paint, which is used extensively on both spacecraft and rocket bodies for thermal control reasons, can deteriorate severely in space, sometimes in a matter of only a few years. The potential magnitude of the problem was not fully recognized until the 1983 flight of the STS-7 Space Shuttle mission, when an impact crater on an orbiter window was apparently caused by a paint chip smaller than a millimeter in diameter. Subsequent analyses of spacecraft components returned from LEO have

confirmed the presence of a large population of paint particles, even though the orbits of individual particles decay quite rapidly.

Perturbation Forces affecting Space Objects

Once in orbit, debris is affected by perturbing forces that can alter its trajectory and even remove it completely from orbit. Other than the gravitational attraction of the Earth, the primary forces acting on a space object in lower orbits (below about 800 km) are atmospheric drag and gravitational perturbations from the Earth. These gravitational perturbations, however, although affecting some orbital parameters, do not generally strongly affect orbital lifetime. For space objects in higher orbits, solar and lunar gravitational influences become more important factors. Small debris can also be affected by solar radiation pressure, plasma drag, and electrodynamics forces, although the effects of plasma drag and electrodynamics forces are typically dwarfed by the effects of solar radiation pressure.

The rate at which a space object loses altitude is a function of its mass, its average cross-sectional area impinging on the atmosphere, and the atmospheric density. Although the Earth's atmosphere technically extends to great heights, its retarding effect on space objects falls off rapidly with increasing altitude. Atmospheric density at a given altitude however, is not constant and can vary significantly (particularly at less than 1,000 km) due to atmospheric heating associated with the 11-year solar cycle. This natural phenomenon has the effect of accelerating the orbital decay of debris during periods of solar maximum (increased sun-spot activity and energy emissions). During the last two peaks in the solar cycle, the total cataloged space object population actually declined, because the rate of orbital decay exceeded the rate of space object generation via new launches and fragmentations.

Figure 8.11, which displays the predicted orbital lifetimes for a number of different objects in circular LEOs at different periods in the solar cycle, illustrates the importance of cross-sectional-area-to-mass ratio, altitude, and solar activity in determining orbital lifetimes in LEO. First, objects with low ratios of cross-sectional area to mass decay much more slowly than objects with high area- to-mass ratios. Second, objects at low altitude experience more rapid orbital decay than objects at high altitude. Finally, objects decay much more rapidly during periods of solar maximum than during the solar minimum.

The combination of all of these forces has caused approximately 16,000 cataloged objects to reenter the atmosphere since the beginning of the space era. In recent years, an average of two to three space objects large enough to be cataloged (as well as numerous smaller debris particles) reenter the Earth's atmosphere each day. Over the course of a year, this amounts to hundreds of metric tons of material. This material is composed primarily of large objects that were launched into low orbits (most of the mass is in the form of large multiton rocket bodies) and small objects with high cross-sectional-area-to-mass ratios. Seldom do any larger objects initially placed into orbits higher than 600 km reenter the atmosphere.

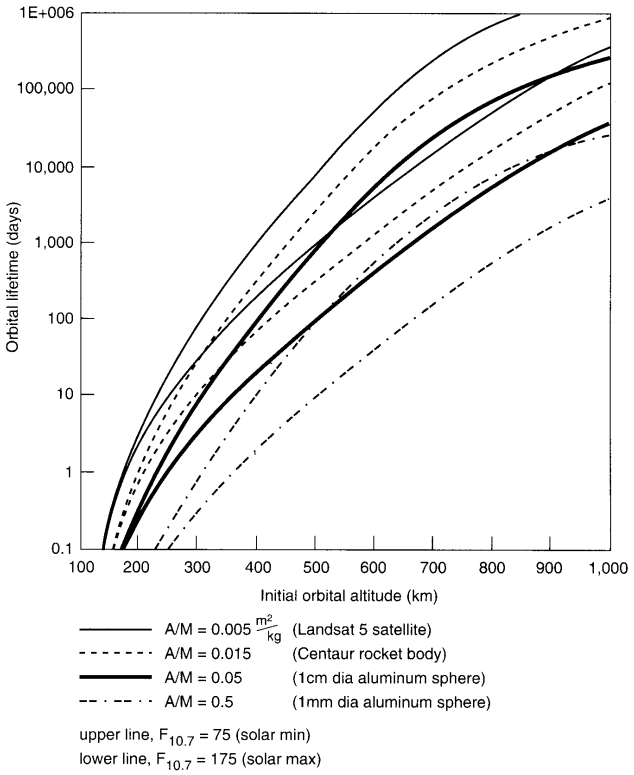

Figure 8.11. Orbital decay time versus altitude

2 Hypervelocity Impacts

The kinetic energy of particles moving at speeds of 10-15 km/sec is roughly equivalent to the energy released by the explosion of 40 times its mass of TNT. For example, a 1 cm diameter aluminum sphere (whose mass is about 1.4 gr.) moving at 13 km/sec has a kinetic energy equivalent to the energy released by the explosion of 56gr. of TNT (about 0.24 MJ). The characteristic of a hypervelocity collision depends on the initial speed as shown.

speed v (km/sec)	
$v < 2$	Projectile remains intact
$2 < v < 7$	Projectile shatters into fragments
$7 < v < 11$	Projectile melts upon impact
$v > 11$	Projectile may vaporize

In addition some fraction of the available energy will be dissipated in generating a crater in the target material. If the crater is sufficiently deep the target material may be penetrated as indicated by the following empirical relationship for the penetration depth t (in cm).

$$t(\text{cm}) = k\, M_p^{\alpha/3}\, \rho_t^{\beta/3}\, v_\perp^{\gamma/3} \qquad \text{(Eqn. 8.10)}$$

M_p = mass of projectile (in gr.)
ρ_t = density of target material (in gr./cm^3)
$v_\perp$ = Projectile velocity component perpendicular to the surface (in km/sec)
k = material specific constant

The constants α, β and γ are empirically determined and on the order of $\alpha \sim 1$, $\beta \sim \frac{1}{2}$ and $\gamma \sim 2$. Results from the Long Duration Exposure Facility (LDEF) have yielded the following expressions for the penetration depth in aluminum.

$$t(\text{cm}) = 0.72\, M_p^{0.352}\, \rho_t^{1/6}\, v_\perp^{0.875} \qquad \text{(Eqn. 8.11)}$$

There also exists an approximate relation for crater depth when the target material is not penetrated. In that case the crater depth P (cm) is

$$t(\text{cm}) = 0.42\, M_p^{0.352}\, \rho_t^{1/6}\, v_\perp^{2/3} \qquad \text{(Eqn. 8.12)}$$

Both of the above relations are illustrated in Fig 8-12 below for an aluminum target surface and a 10 km/sec incident projectile.

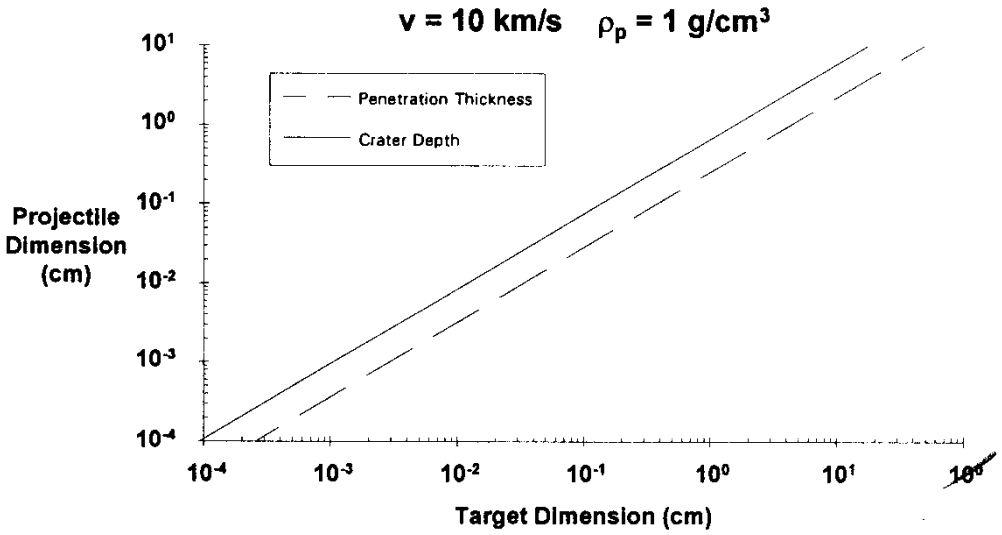

Figure 8.12. Crater diameter and penetration thickness in aluminum

As was shown in the previous section the effects of orbital debris collision range from surface degradation all the way to catastrophic destruction of the spacecraft. For a given projectile dimension (and speed) the crater formed in a block of material is less deep than the thickness of a flat plate penetrated. This effect is due to spallation and shockwave reflection from the back surface of the plate.

3 Impact Probabilities.

A number of complex models have been constructed to predict the flux of orbital debris objects as a function of debris mass (or size) and altitude. The results of one such projection is shown in Figure 8-13.

To calculate the impact probability we must first find N the number of impacts in time T which is given by

$$N = \int_{t}^{t+T} FA \, dt \qquad \text{(Eqn. 8.13)}$$

where F =Flux (Particles/m^2/year are the usual units); A = Surface area (m^2)
Once we have N we can obtain the probability of n impacts from the well-known Poisson distribution as:

$$P_n = \frac{N^n}{n!} e^{-N} \qquad \text{(Eqn. 8.14)}$$

To estimate the number of impacts due to objects greater than a specific mass we exclude the lower mass particles from the flux in calculating N.

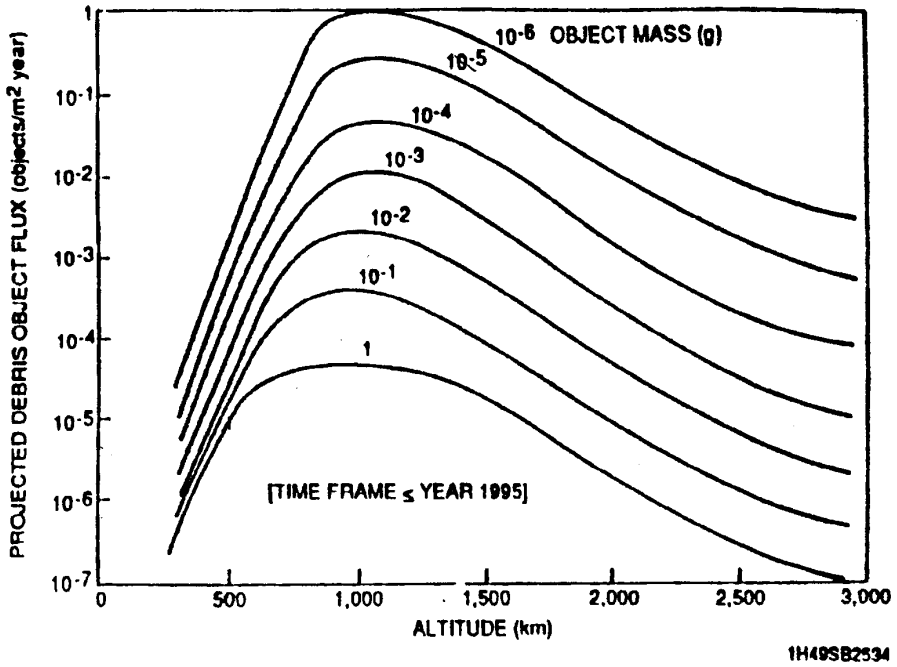

Figure 8.13 1995 Space Debris Projection

Although the Orbital Debris environment is not well defined or understood a number of models have been constructed which approximate the flux F for specified particle diameter, orbital altitude, solar activity index, orbital inclination, year of observation and assumed debris growth and decay rates.

Figure 8.14 shows the results for a typical LEO orbit and specified conditions

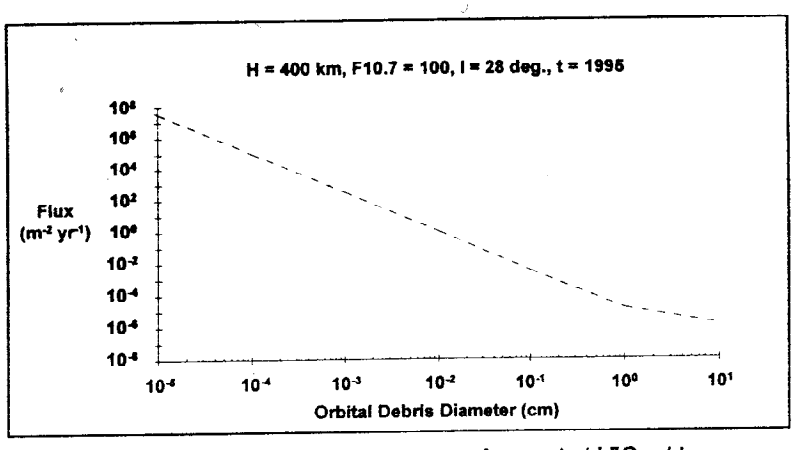

Figure 8.14

Suppose we wish to calculate the probability for 0,1 and 2 impacts of a 1mm projectile on a spacecraft of $5m^2$ surface area in one year

$$N = \int_0^1 FAdt = 5x10^{-2} \qquad \text{(Eqn. 8.15)}$$

using the Poisson distribution we obtain

$$P_0 = \frac{N^0}{0!}e^{-N} = e^{-N} = e^{-0.05} = 0.9512$$
$$P_1 = \frac{N^1}{1!}e^{-N} = 0.05e^{-0.05} = 0.0475 \qquad \text{(Eqn. 8.16)}$$
$$P_2 = \frac{N^2}{2!}e^{-N} = \frac{(.05)^2}{2}e^{-0.05} = 0.0012$$

as the probabilities for 0,1 or 2 impacts/year

4 Design Considerations

Spacecraft thermal blankets or structural panels can provide adequate shielding for small (diameter < .1mm) debris. For larger debris orienting sensitive surfaces away from ram direction or flying at altitudes or orbital inclinations that minimize debris flux can be helpful.

Considerable work on debris "bumpers" is currently underway. These bumpers consist of multiple sheets of material separated by few centimeters. The space between them may be empty or filled with materials such as Kevlar or Nextel. The outer shield is expected to be penetrated by the incident particle, but the impact would fragment the projectile into many smaller pieces which would then be stopped by the back layer of the bumper.

C Surface Effects

1 Atomic Oxygen Effects

At 300 km altitude ambient atmospheric density is about ten orders of magnitude below that encountered at sea level. However there are still ~10^{15} oxygen atoms/m^3 and $1m^2$ spacecraft orbiting at 8 km/sec will undergo about 10^{19} collisions with ambient atoms/sec with an effective collision energy of about 5eV. Since atomic oxygen is highly reactive these collisions result in oxidation and erosion of surface materials.

Consider the erosion of material from a surface due to a flux of oxygen atoms. The mass loss in time dt is given by

$$dm = \rho(RE) \varnothing A \, dt \qquad \text{(Eqn. 8.17)}$$

where: ρ(gr./cm^3) is the material density
$\varnothing$ (OA atoms/cm^2-sec) is the atomic oxygen flux
(RE) is the reaction efficiency in units (cm^3/OA atom).
The reaction efficiency is an experimentally determined quantity, which may be a function of various parameters such as surface temperature, uv flux, atomic oxygen flux, etc.

The above equation can also be rewritten to show the rate of change of thickness of the target.

$$\frac{dx}{dt} = (RE) \varnothing \left(\text{cm} \diagup \text{sec} \right) \qquad \text{(Eqn. 8.18)}$$

This rate of change can be as high as a few tenths of a millimeter per year for certain thermal control materials such as kapton.

Table 8.3 Atomic Oxygen Reaction Efficiency - Reaction Efficiency x 10^{-24} cm^3/atom

Material	Range	Best Value
Aluminum	-	0.00
Carbon	0.9-1.7	-
Epoxy	1.7-2.5	-
Fluoropolymers		
-FEP Kapton	-	0.03
-Kapton F	-	<0.05
-Teflon, FEP	-	<0.05
-Teflon	0.03-0.50	-
Gold	-	0.0
Indium Tin Oxide	-	0.002
Mylar	1.5-3.9	-
Paint		
-S13GLO	-	0.0
-YB71	-	0.0
-Z276	-	0.85
-Z302	-	4.50
-Z306	-	0.85
-Z853	-	0.75
Polyimide		
-Kapton	1.4-2.5	-
-Kapton H	-	3.04
Silicones		
-RTV560	-	0.443
-RTV670	-	0.0
Silver	-	10.5
Tedlar		
-Clear	1.3-3.2	-
-White	0.05-0.6	-

It should also be kept in mind that significant changes in the thermal and optical properties of surfaces can occur without appreciable mass loss.

Another very important effect is the deterioration of interconnects between solar cells which are often made of silver. If unprotected these connecting wires may literally be worn away and the solar array may fail.

2 UV Degradation

Essentially all solar radiation below 0.3mm in wavelength is absorbed by the atmosphere before it reaches the surface of the earth. A satellite on the other hand is exposed to the full spectrum of solar radiations including UV and X Rays. The photon energy corresponding to l = 0.3 μm is about 4 eV. As the table shows typical UV photon energies are sufficient to break many chemical bonds and thereby alter the physical properties of surfaces.

Table 8.4 - Chemical Bond Energy

Chemical	Bond	Bond Energy at 25 degrees C (kcal/mole)	Bond Energy at 25 degrees C (eV)	Wavelength (microns)
C-C	Single	80	3.47	0.36
C-N	Single	73	3.17	0.39
C-O	Single	86	3.73	0.33
C-S	Single	65	2.82	0.44
N-N	Single	39	1.69	0.73
O-O	Single	35	1.52	0.82
Si-Si	Single	53	2.30	0.54
S-S	Single	58	2.52	0.49
C-C	Double	145	6.29	0.20
C-N	Double	147	6.38	0.19
C-O	Double	176	7.64	0.16
C-C	Triple	198	8.59	0.14
C-N	Triple	213	9.24	0.13
C-O	Triple	179	7.77	0.16

One of the important quantities for thermal control of spacecraft is the solar absorptance α_s which varies from 0 for perfect reflector to 1 for a perfect absorber. Large changes in the absorptance (on the order of 50%) have been observed due to UV irradiation for certain materials and exposure times on the order of 1000 hrs.

3 Sputtering

When atoms or ions of sufficient energy impact a solid surface they can eject atoms in a process called sputtering. In Table 8.5 are listed the minimum energies which an incident particle must have to cause sputtering on various target materials.

Table 8.5 - Sputtering Thresholds - Bombarding Gas Threshold (eV)

Target Material	O	O_2	N_2	Ar	He	H
Ag	12	14	13	17	25	83
Al	23	29	27	31	14	28
Au	19	15	15	15	53	192
C	65	82	79	88	40	36

Cu	15	22	21	24	20	60
Fe	20	28	27	31	23	66
Ni	20	29	27	31	24	72
Si	31	39	37	42	18	40

The energies which are available in collisions between atmospheric atoms and moving satellite surface are generally lower than the sputtering thresholds. Thus collisions due to the orbital motion of the satellite do not cause a significant amount of sputtering.

However we did see earlier that satellite surfaces can become negatively charged up to several kilovolts and these negatively charged surfaces will accelerate any positive ions in the atmosphere toward the surface yielding impact energies of hundreds or even thousands of eV more than enough to cause sputtering as shown in Table 8.6 below for the case of 100eV incident particles on various target surfaces.

Table 8.6 - Sputtering Yields (atoms/particle) at 100eV Impact Energy

Target Material	O	O2	N2	Ar	He	H
Ag	0.265	0.498	0.438	0.610	0.030	-
Al	0.026	0.076	0.060	0.110	0.020	0.010
Au	0.154	0.266	0.244	0.310	-	-
C	-	-	-	-	0.008	0.008
Cu	0.385	0.530	0.499	0.600	0.053	-
Fe	0.069	0.153	0.129	0.200	0.028	-
Ni	0.120	0.247	0.239	0.270	0,029	-
S	0.029	0.054	0.046	0.070	0.023	0.002

On extended missions the sputtering of materials, in particular metals can cause erosion as well as changes in surface properties.

4 Molecular Contamination

Many materials when placed in a vacuum will "outgas" meaning that atoms or molecules will spontaneously leave the surface. In space outgassing materials may deposit contaminants onto sensitive surfaces such as thermal control panels, solar arrays or optical surfaces thereby altering their thermal or optical properties. To make matters worse we sometimes observe synergistic effects which result in total degradation which is greater than the sum of its parts. One such example is the interaction of solar UV with contamination films deposited by outgassing. By polymerizing the contaminant molecules films can be made to adhere to warm surfaces such as solar panels. An example of this effect is shown in the graph below.

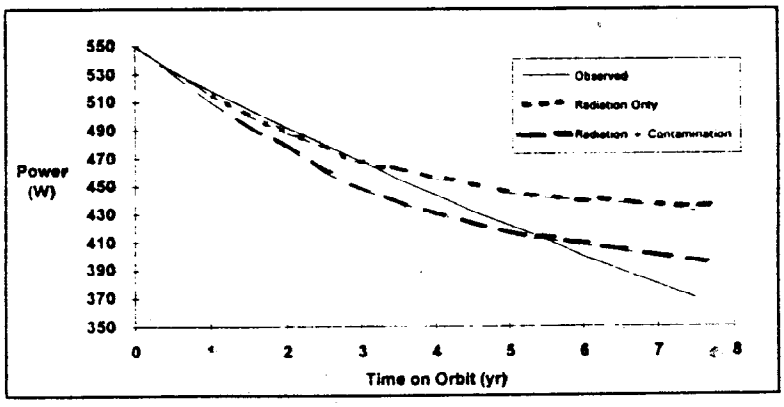

Fig. 2.12 GPS Block I solar power degradation.
(©1991 AIAA—reprinted with permission)

Figure 8.15

D Homework

1. Using the formula for attracted and repelled species, plot the magnitudes (absolute values) of the ion and electron currents to a satellite for the following parameters:
proton plasma: ion mass = 1.67×10^{-27} kg
ion temperature: ~~20 keV~~
electron temperature: ~~20 keV~~ use T = 5 KeV for ions and electrons
electron density = 1×10^{6} m^3
Φ = 0 to -20 kV

note the formula to be using are: $I = I_o e^{-q\Phi/kT}$ (Eqn. 8.7a) and $I = I_o \left(1 - \frac{q\Phi}{kT}\right)$ (Eqn. 8.7b).

$I_o = q\ n\ v$; $v = \sqrt{\frac{kT}{m}}$;
The charge q will be positive for ions, and negative for electrons
($e = 1.6 \times 10^{-19}$, $m_e = 9.1 \times 10^{-31}$)
Assume the satellite has a surface area of 1 m^2.

The two curves will intersect. The intersection point is where the net current is zero, and hence the equilibrium point.